

## ARTICLE

Received 2 May 2014 | Accepted 29 Sep 2014 | Published 12 Nov 2014

DOI: 10.1038/ncomms6411

# Unencapsulated *Streptococcus pneumoniae* from conjunctivitis encode variant traits and belong to a distinct phylogenetic cluster

Michael D. Valentino<sup>1,2,3</sup>, Abigail Manson McGuire<sup>3</sup>, Jason W. Rosch<sup>4</sup>, Paulo J.M. Bispo<sup>1,2</sup>, Corinna Burnham<sup>4</sup>, Christine M. Sanfilippo<sup>5,†</sup>, Robert A. Carter<sup>4</sup>, Michael E. Zegans<sup>6</sup>, Bernard Beall<sup>7</sup>, Ashlee M. Earl<sup>3</sup>, Elaine I. Tuomanen<sup>4</sup>, Timothy W. Morris<sup>5,†</sup>, Wolfgang Haas<sup>1,2</sup> & Michael S. Gilmore<sup>1,2,3</sup>

*Streptococcus pneumoniae*, an inhabitant of the upper respiratory mucosa, causes respiratory and invasive infections as well as conjunctivitis. Strains that lack the capsule, a main virulence factor and the target of current vaccines, are often isolated from conjunctivitis cases. Here we perform a comparative genomic analysis of 271 strains of conjunctivitis-causing *S. pneumoniae* from 72 postal codes in the United States. We find that the vast majority of conjunctivitis strains are members of a distinct cluster of closely related unencapsulated strains. These strains possess divergent forms of pneumococcal virulence factors (such as CbpA and neuraminidases) that are not shared with other unencapsulated nasopharyngeal *S. pneumoniae*. They also possess putative adhesins that have not been described in encapsulated pneumococci. These findings suggest that the unencapsulated strains capable of causing conjunctivitis utilize a pathogenesis strategy substantially different from that described for *S. pneumoniae* at other infection sites.

<sup>1</sup>Department of Ophthalmology, Massachusetts Eye and Ear Infirmary, 243 Charles Street C703, Boston, Massachusetts 02114, USA. <sup>2</sup>Department of Microbiology and Immunobiology, Harvard Medical School, 77 Avenue Louis Pasteur, Boston, Massachusetts 02115, USA. <sup>3</sup>The Broad Institute of MIT and Harvard, 320 Charles Street, Cambridge, Massachusetts 02141, USA. <sup>4</sup>Department of Infectious Diseases, St. Jude Children's Research Hospital, 262 Danny Thomas Pl., Memphis, Tennessee 38105, USA. <sup>5</sup>Bausch and Lomb Inc., 1400 Goodman Street North, Rochester, New York 14609, USA. <sup>6</sup>Department of Microbiology and Immunology, Geisel School of Medicine at Dartmouth, 1 Rope Ferry Road, Hanover, New Hampshire 03755, USA. <sup>7</sup>Streptococcus Laboratory, Centers for Disease Control and Prevention, 1600 Clifton Road, Atlanta, Georgia 30333, USA. † Present address: Upstate Stem Cell cGMP Facility, University of Rochester, 601 Elmwood Avenue, Rochester, New York, 14642, USA (C.M.S.); Actelion Clinical Research, 1820 Chapel Avenue, Cherry Hill, New Jersey 08002, USA (T.W.M.). Correspondence and requests for materials should be addressed to M.S.G. (email: michael\_gilmore@meei.harvard.edu).

*Streptococcus pneumoniae* is a leading cause of invasive infections including pneumonia, meningitis and sepsis, as well as noninvasive infections including pharyngitis and otitis media. The polysaccharide capsule, a key virulence factor, is the target of current vaccines<sup>1–3</sup>. Vaccination has substantially reduced morbidity and mortality<sup>3</sup> but has had limited impact on conjunctivitis, infection of the mucous membrane covering the eye and lining the eyelids<sup>4</sup>.

We recently collected 271 *S. pneumoniae* isolates during the course of clinical trials for the treatment of bacterial conjunctivitis<sup>5–7</sup> and found that over 90% were unencapsulated<sup>8</sup>, and hence unaffected by current vaccine design. Unencapsulated *S. pneumoniae* strains have caused large conjunctivitis outbreaks in schools and colleges<sup>9–13</sup>, military training facilities in the United States<sup>14</sup> and at other locations worldwide<sup>15</sup>. Recent outbreaks have involved one multilocus sequence type (MLST) in particular, ST448 (ref. 13). However, a previous study of epidemiologically unrelated conjunctivitis cases found that most cases were caused by encapsulated strains<sup>4</sup>. That study examined isolates before the widespread use of the PCV7 vaccine introduced in 2000 (ref. 4).

With a view towards assessing the impact of the vaccine and improved vaccine design, and to better understand the diversity of strains and genetic basis for *S. pneumoniae* pathogenesis in conjunctivitis, here we describe the results of an extensive comparative analysis of *S. pneumoniae* currently associated with conjunctivitis.

## Results

**Epidemiology of conjunctivitis.** To determine the diversity of *S. pneumoniae* causing conjunctivitis, 271 strains<sup>5–8</sup> were characterized by MLST<sup>16</sup> (Fig. 1, Supplementary Data 1). Sequence type ST448 (refs 17,18) was found to cause the majority of infections (67.2%). The next most common types caused substantially fewer: ST344 (8.9%), ST1186 (4.8%) and ST2315 (4.4%). Together, 10 different sequence types of unencapsulated *S. pneumoniae* accounted for 90.8% of conjunctivitis cases. A diverse set of strains of *S. pneumoniae* from other types of infections, for which closed genomes are available in Genbank, were included for comparison (Supplementary Data 2). A distinct, deeply rooted cluster of *S. pneumoniae* was formed that included 11 unencapsulated MLST types encompassing 89.3% of conjunctivitis isolates (Fig. 2). Only one sequence type that is encapsulated, ST199, caused more than two cases. This shows that conjunctivitis in the United States is mainly caused by a closely related group of unencapsulated *S. pneumoniae* sequence types, although other strains can cause conjunctivitis, most likely as an extension of upper respiratory infection.

**Traits of the unencapsulated conjunctivitis cluster.** To determine whether strains from conjunctivitis that occur within the distinct branch of *S. pneumoniae* possess novel gene content, a total of 21 genomes of representatives of the major conjunctivitis-associated sequence types were sequenced (Supplementary Data 3). Diversity was maximized by selecting varying dates of isolation and sites of origin. In addition, genomes of select encapsulated conjunctivitis strains were also sequenced, including ST199 (which caused five cases) and strains of sequence types ST632, ST667 and ST180.

Genes encoding a total of 4,433 protein orthogroups were identified by OrthoMCL, 1,160 of which were present in single copy in all genomes. These core orthogroup genes were used to generate a single-nucleotide polymorphism (SNP)-based phylogenetic tree (Fig. 3). As for MLST, the SNP-based core genome tree showed that strains isolated from epidemic conjunctivitis

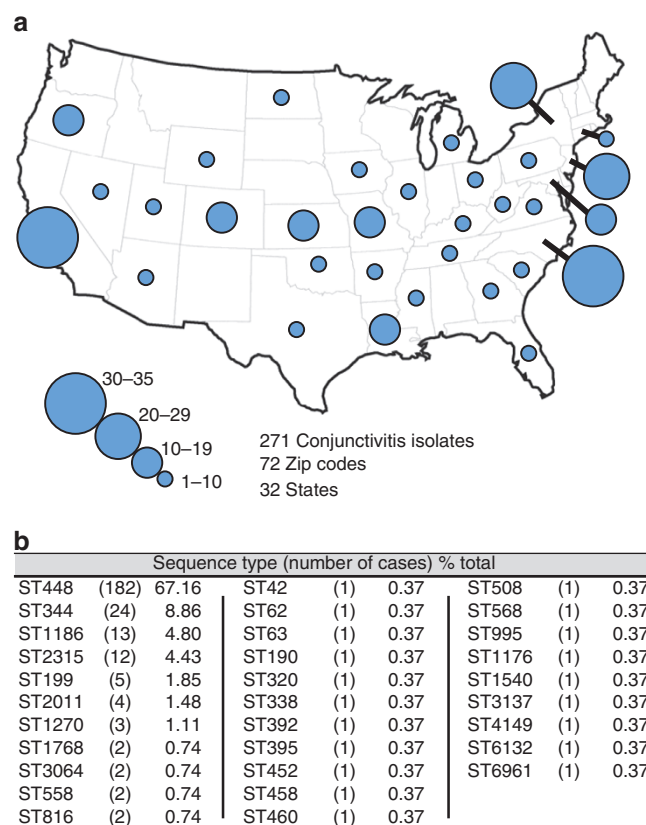


**Figure 1 | Location and MLST profile of conjunctivitis isolates.** Two hundred seventy-one isolates of *S. pneumoniae* from diagnosed cases of conjunctivitis. (a) Number and geographic location of isolates. (b) Frequency of MLST types among conjunctivitis isolates.

belong to a distinct, deeply resolved group that includes ST448, ST1186, ST344, ST1270 and ST2315. Lineages within this group were termed the epidemic conjunctivitis cluster (ECC), since their genomes are highly related and these STs (ST448, ST344 and ST1186) are associated with epidemic conjunctivitis outbreaks<sup>9,10,14,17,18</sup>. Croucher *et al.*<sup>19</sup> recently noted that one group of unencapsulated strains (denoted Sequence Cluster 12 (SC12)) was the most divergent cluster from the main population in their study. SC12 includes STs ST448 and ST344 associated with conjunctivitis. The phylogeny determined here was unchanged after filtering recombinogenic regions of DNA using BRAT NextGen<sup>20</sup>, showing that recombination was not the main driver for this population structure. Encapsulated strains that are rarer causes of conjunctivitis (ST632, ST667, ST180 and ST199) are interspersed among strains that cause infection at other sites. The extent of divergence of shared genes within ECC genomes from those of other sites of infection was quantified<sup>21</sup> (Supplementary Fig. 1). ECC genomes compared with each other exhibit an average nucleotide identity (ANI) value of 99.0%  $\pm$  0.4, highlighting the very close relationship among ECC lineages. ECC strains are significantly more distantly related to those from other sites of infection (97.9%  $\pm$  0.11 ANI,  $P$  < 0.001, Student's *t*-test).

**ECC strains possess a distinct gene repertoire.** Clustering of genomes based on similarities in gene content also places ECC strains into a well-resolved group, independently recapitulating phylogenetic structure (Supplementary Fig. 2) and supporting the hypothesis that the peculiar ocular tropism of ECC strains stems

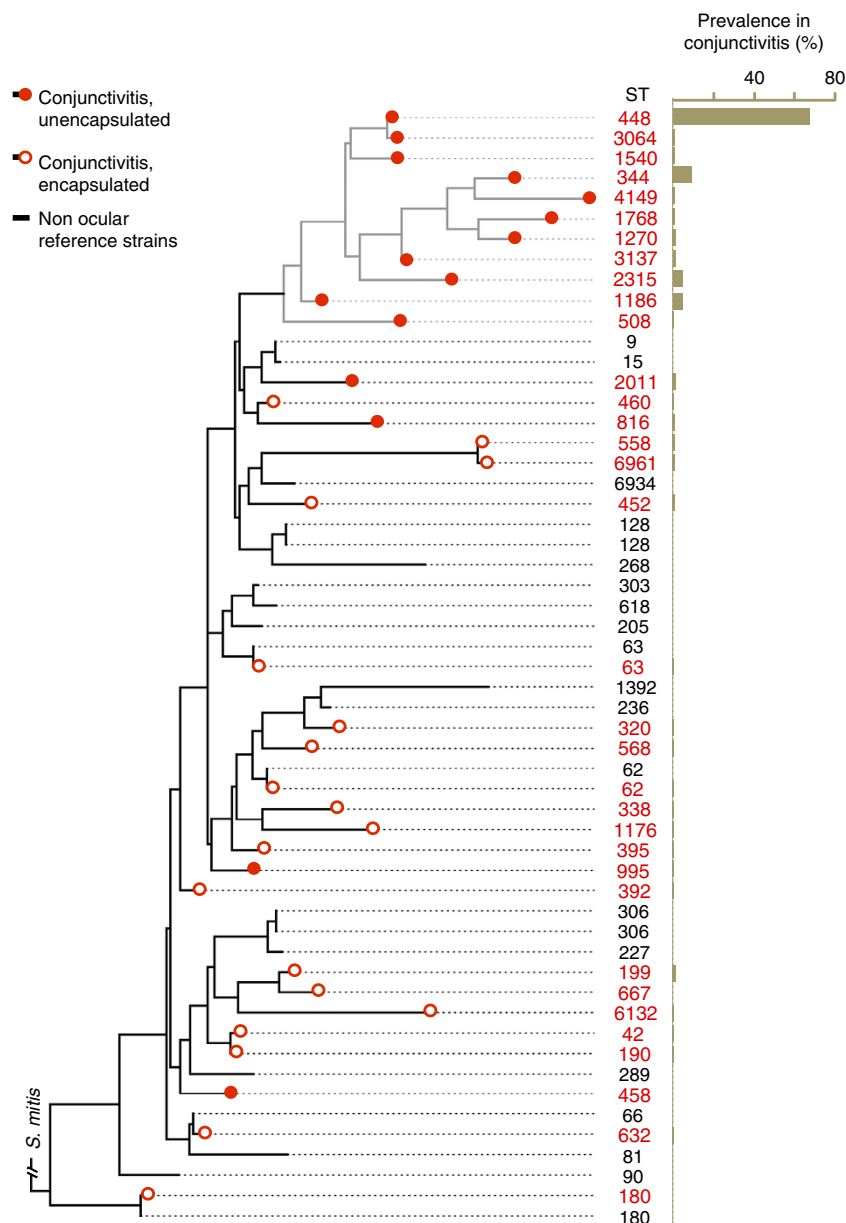


**Figure 2 | MLST-based phylogenetic relationships among conjunctivitis strains.** SNP-based tree based on a concatenation of MLST loci, with prevalence in conjunctivitis for each ST.

at least in part from novel gene content. As in the SNP-based phylogeny, strains that are rarer causes of conjunctivitis are interspersed among non-ocular *S. pneumoniae*. To identify genes that distinguish the ECC from other strains, because horizontal gene flow can complicate the analysis, we arbitrarily set gene presence in 80% or greater of ECC genomes, and <20% of the non-ECC comparator strains (or *vice versa*) as the cutoff. We found 230 genes that fulfil this enrichment criteria (Supplementary Data 4). Of these, 103 genes are in all ECC genomes and absent from all comparators. Conversely, 70 genes are missing from ECC that are present in 80–100% of non-ocular *S. pneumoniae* comparator genomes (Supplementary Data 5). Of those, 29 were found in all non-ocular genomes and no ECC strains. In patterns of gene presence and absence, encapsulated conjunctivitis strains were found to be most closely associated with those from other types of infection.

The comparatively large proportion of conjunctivitis caused by ST448 suggests that its genome may be especially refined to cause

this disease (or alternatively, that among ECC lineages, ST448 is more widely distributed and abundant in nature). Seventeen orthogroups are unique to ST448 (Supplementary Data 6), including a hypothetical mobile element with closest relative in *S. mitis*. No genes are specifically missing from ST448 that are in all other ECC genomes.

**Evidence for large-scale surface remodelling.** In place of a capsule operon, all ECC strains we investigated possess the atypical locus that includes *aliC* (X231\_0947) and *aliD* (X231\_0948) but not the often-associated *pspK* gene<sup>22,23</sup>. However, in the absence of a capsule, a large number of novel surface features were found. Exclusive to ECC are two different Antigen I/II family adhesins (X231\_1085 and X231\_1187; Supplementary Data 4) that appear to originate from *S. macedonicus* and *S. mitis*, respectively (Fig. 4a). Owing to the presence of multiple SspB domains within these proteins, we termed them SspBC1

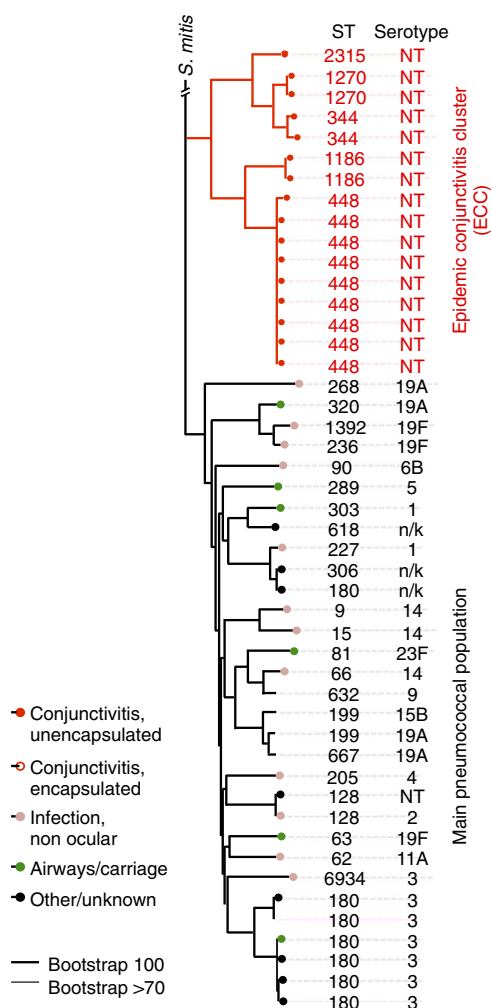


**Figure 3 | ECC strains belong to a well-resolved group of the species *S. pneumoniae*.** A PhyML SNP-based tree based on the concatenated alignments of 1,160 single-copy core genes (for strain identities, see Supplementary Data 2). Bootstrapping was performed with 1,000 iterations.

(X231\_1085) and SspBC2 (X231\_1187). SspB domain-containing proteins have been shown to bind the human scavenger protein gp-340, which contributes to bacterial aggregation<sup>24</sup>. To test for this functionality, a representative ECC strain (ST448), and a non-ECC-encapsulated conjunctivitis strain that lacks SspBC1 and SspBC2 (ST199), were incubated with graded concentrations of gp-340. As shown in Fig. 4b, the ST448 strain exhibited gp-340 concentration-dependent aggregations. We also identified a unique gene inferred to encode a surface protein (X231\_1186) termed here PspO. This surface protein gene is directly adjacent to that encoding SspBC2, suggesting a potential virulence island. PspO includes a C-terminal glucan-binding domain and a surface exclusion domain.

Another gene predicted to affect the host/pathogen interface, that occurs exclusively in ECC strains, encodes a new divergent putative zinc metalloprotease (X231\_0594), ZmpC2 (Supplementary Fig. 3A). The closest orthologue is in *S. pseudopneumoniae* IS7493, and it shares 31% amino-acid sequence identity with the known ZmpC of *S. pneumoniae*, mainly in the Peptidase\_M26\_C domain (Supplementary Fig. 3A). Recently, a different, structurally related, atypical zinc metalloprotease C (*zmpC*, now termed ZmpC1) was identified in a *S. pneumoniae* conjunctivitis isolate, and was shown to cleave

mucins from corneal epithelial cells<sup>25,26</sup>. ZmpC1 (X231\_0222) also occurs in 100% of ECC and 0% of comparators.

Additional surface-related functions of potential relevance to conjunctivitis include a putative sialidase (X231\_0534), now termed NanO1. It shares 88% amino-acid sequence identity with sialidase A (neuraminidase A) of *S. pseudopneumoniae*. The typical NanA of *S. pneumoniae*, which is carried by all non-ocular reference strains, has been displaced by NanO1 in ECC (Supplementary Fig. 3B). Closer examination of the sequence surrounding *nanO1* identifies a second gene, also annotated as encoding a sialidase (referred to as NanO2, X231\_0533), suggesting that NanO1 and NanO2 from *S. pseudopneumoniae* recombinationally displaced wild-type NanA (Supplementary Fig. 3C). In addition, the neuraminidase allele NanC, found in ~51% of *S. pneumoniae* isolates from non-ocular sites<sup>27</sup>, was not found within any ECC genome.

Choline-binding proteins (Cbps) are important virulence factors that contribute to *S. pneumoniae* adhesion and transcytosis<sup>28</sup>. All ECC genomes encode a novel, divergent Cbp (BM49\_0273), CbpI1, that is most closely related to a variant in *S. pseudopneumoniae*. All ECC strains also encode a second Cbp variant (X231\_0220, CbpI2) that is rare outside this cluster, occurring in three non-ocular comparator strains (AP200, G54 and TIGR4)<sup>28</sup>. CbpI1 and CbpI2 share a structurally related cysteine-rich secretory domain and a C-terminal choline-binding domain, and 48.3% overall amino-acid sequence identity. Interestingly, CbpI2 and ZmpC1 are adjacent to one another within the ECC genomes.

*S. pneumoniae* genes with known roles in colonization and virulence include *cbpA*, *nanB*, *bgaA*, *strH*, *ply*, *hyl*, *plpA* (*aliA*), *psaABC*, *prtA*, *choP*, *pdgA*, *adr*, *spxB*, *amiA-amiF*, *msrA/B2* and the two Pilus Islets<sup>29–31</sup>. Choline-binding protein A (CbpA), a main adhesin in respiratory infections and otherwise highly conserved in non-ocular strains<sup>31,32</sup>, is substantially divergent in all ECC genomes. Two polymorphic forms of CbpA were found, CbpAC1 in ST448 and ST1186 genomes, and CbpAC2 in ST344, ST1270 and ST2315 (Fig. 5). Portions of CbpAC1 and CbpAC2 show little resemblance to CbpA, instead being closely related to the beta antigen of *S. agalactiae*<sup>33</sup>. The absence of CbpA from ECC strains was verified with western blot analysis using three different CbpA-specific monoclonal antibodies<sup>34</sup>, indicating that the variant CbpA possesses a substantially different structure in the otherwise conserved key epitopes probed (Supplementary Fig. 4). The region of canonical CbpA that mediates binding to the eukaryotic polymeric Ig receptor<sup>35</sup> has been replaced by *S. agalactiae* domains that bind the Fc portion of IgA directly<sup>33,36</sup>. The different variations in the divergence of CbpAC1 and CbpAC2 from CbpA suggest that variations of the hybrid CbpA locus evolved independently. Interestingly, in ECC the two-component system that regulates CbpA expression<sup>37</sup> also exhibits greater nucleotide sequence identity to its counterpart in *S. agalactiae* (Supplementary Fig. 4D). Differences in nucleotide sequence on either side of the two variant CbpAC loci support separate evolution of these determinants within ECC strains.

Two pilus islets have been described that contribute to *S. pneumoniae* epithelial cell adhesion<sup>29,30</sup>. Neither pilus islet occurred in any ECC strain. Exoglycosidase BgaA is absent from all ECC isolates, as is a three-gene phosphotransferase system (PTS) (SP\_0645 to SP\_647) that occurs immediately adjacent to *bgaA* in TIGR4, displaced by ~1 kb of sequence with high identity (>91%) to sequences in *S. mitis* and *S. pseudopneumoniae*. Otherwise, all other virulence-associated genes, including *nanB*, *strH*, *ply*, *hyl*, *plpA* (*aliA*), *psaABC*, *prtA*, *choP*, *pdgA*, *adr*, *spxB*, *amiA-amiF* and *msrA/B2* are present in all ECC strains, and are highly conserved (99.6% ± 0.3 inferred amino-acid sequence identity to TIGR4).

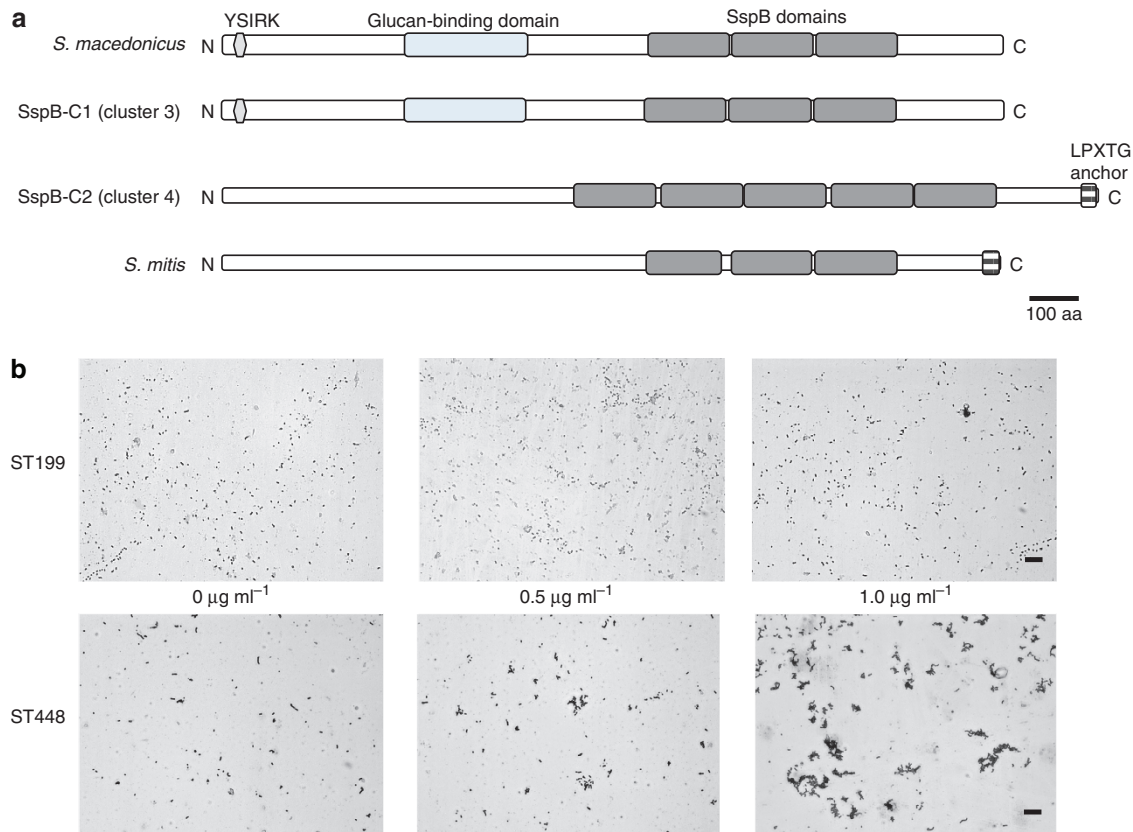


**Figure 4 | Homologues of agglutinin receptors in ECC.** (a) SspBc1 and SspBc2 agglutinins exhibit identity to glucan-binding and SspB domains in orthologues from *S. macedonicus* or *S. mitis*. (b) Aggregation of ST448 (ECC\_3540) and ST199 (SC\_3526) isolates after addition of 0.5 and 1.0  $\mu\text{g ml}^{-1}$  of gp-340 visualized with Gram staining. Scale bar represents 20  $\mu\text{m}$ .

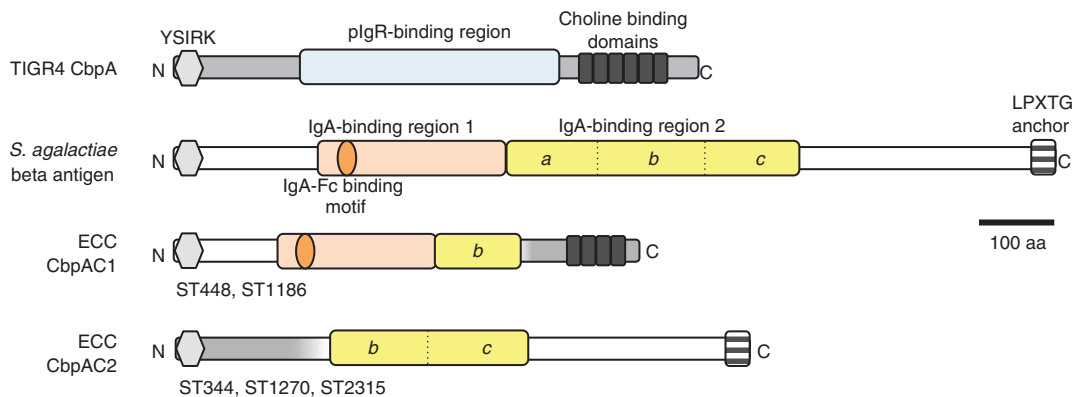


**Figure 5 | ECC genomes encode an atypical CbpA.** Canonical CbpA of TIGR4 compared with those in ECC genomes, and the inferred donor, *S. agalactiae* beta antigen. Sequence most likely deriving from *S. pneumoniae* (grey) and *S. agalactiae* (white). Domains relevant to polymeric Ig receptor (pIgR) or IgA-binding are highlighted. The IgA-binding domain of *S. agalactiae* beta antigen is duplicated, and domain 2 has been divided into portions (a, b, c) for purposes of illustrating the likely origins of fragments that share amino-acid sequence identity in ECC variants.

**Metabolic differences.** All ECC strains encode a putative phosphoenolpyruvate-dihydroxyacetone phosphotransferase system (X231\_1297 to X231\_1300, Supplementary Data 4). Uniformly absent from ECC strains are operons for arginine metabolism (SP\_2148 to SP\_2151), and a fucose-binding, uptake and catabolic pathway (SP\_2158 to SP\_2170) (Supplementary Data 5). This block of metabolic functions has been displaced in ECC genomes with a 12.7-kb sequence that encodes, among other things, ZmpC2. Some ECC (ST448, ST344 and ST1270) lack the *pia* operon-mediating iron uptake, which in other strains has been linked to virulence in mouse models of pulmonary and

systemic infection<sup>38</sup>. Five other genes with putative annotations as amino-acid transporters (SP\_0111, SP\_0112 and SP\_0709 to SP\_0711) are present in 100% of comparators, but are uniformly absent in ECC, suggesting a substantially altered nutrient profile in the conjunctival mucosa (Supplementary Data 5).

**Recombination and horizontal gene transfer.** The occurrence of multigene blocks of difference suggests that movement of pathogenicity islands or other mobile elements were involved in the evolution of ECC. Of the 230 orthogroups enriched in ECC,

**Table 1 | Gene clusters enriched in ECC genomes.**

Cluster*	Putative function†	Putative origin‡	Size (kb)	% GC
2	Atypical capsule locus of NT pneumococci	<i>S. pneumoniae</i>	6.1	37.9
5	ZmpC1 specific to conjunctivitis genomes, Cbpl2	<i>S. pneumoniae</i>	11.4	38.3
14	ZmpC2	<i>S. pseudopneumoniae</i>	10.2	40.1
3	SspBC1 agglutinin receptor	<i>S. macedonicus</i>	15.4	40.8
4	SspBC2 agglutinin receptor from <i>S. mitis</i> . Unknowns from <i>S. oligofermentans</i> §	<i>S. mitis</i> , <i>S. oligofermentans</i>	17.7	36.4
10	Mobile genetic element§	<i>S. oligofermentans</i>	16.8	35.9
9	Phage§	Non- <i>S. pneumoniae</i> , <i>Streptococcus</i> sp.	18.7	37.0
11	Mobile genetic element containing putative type IV secretory system genes§	<i>S. macedonicus</i>	13.2	42.6
8	Metabolic cassette, triose metabolism	<i>S. pneumoniae</i>	4.4	38.3
1	Phage element, intact, containing toxin/antitoxin in ST448/ST1186	<i>S. pneumoniae</i>	33.4	39.4
6	Lanthionine biosynthesis genes and unknowns from <i>S. oralis</i>	<i>S. oralis</i> , 5', 4.6 kb/ <i>S. pneumoniae</i> , 3'	16.2	29.9
7	ABC-type transport system	<i>S. pneumoniae</i>	4.5	38.0
15	Phage element	<i>S. pneumoniae</i>	10.1	36.6
12	Unknown	<i>S. pneumoniae</i>	4.7	29.2
13	Unknown	<i>S. parasanguinis</i>	1.7	32.2

ECC, epidemic conjunctivitis cluster.

\*The very high-quality ST448 strain ECC\_3510 genome was arbitrarily selected to identify patterns of clustering among the genes of difference in ECC strains. A cluster is defined as two or more contiguous genes.

†Refer to Supplementary Data 4 for full list of genes associated with each cluster.

‡On the basis of highest BLAST result on the nucleotide sequence.

§Clusters that are not found on a single contig but could be linked together by synteny analysis versus a closed reference genome.

180 genes occur in 15 clusters (Table 1). The average G + C content ( $36.8\% \pm 3.8$ ) is lower than the rest of the genome ( $39.7\%$ ,  $P < 0.01$ , Student's *t*-test), which is common for mobile elements<sup>39</sup>. Two clusters exclusive to ECC, an 18-kb predicted phage (cluster 9) and 13-kb encoding core genes (VirD/VirB/TrsE) of a Type IV secretion system (cluster 11), are adjacent. Interestingly, the cluster 9/cluster 11 element occurs at different locations within ECC STs, suggesting either independent acquisition or internal movement. That it is mobile and presumably could be lost if not for selection, yet is retained, suggests that it may have a role in mediating the peculiar ocular tropism of ECC.

The majority (75%) of ECC carry resistance elements (Supplementary Fig. 5) consistent with antibiotic susceptibility<sup>40</sup>. Macrolide resistance is the most common, and is conferred by the Macrolide Efflux Genetic Assembly cassette in ST448 and ST1186, and by a Tn916-like integrative conjugative element in ST344 and ST1270 (Supplementary Fig. 6). ST2315 was the only ECC isolate resistant to phenicols, which was conferred by an Spn11930-like integrative conjugative element element.

### Comparison with strains identified in asymptomatic carriage.

Asymptomatic nasopharyngeal carriage generally precedes disease. To determine whether ECC strains were represented in large data sets from asymptomatic carriage, we looked for their occurrence in two recently reported studies<sup>19,41</sup>. This expanded analysis substantiates the deeply rooted and well-clustered grouping of the ECC strains but, importantly, shows that ECC STs are distributed among additional closely related, unencapsulated strains isolated from the nasopharynxes that have not yet been associated with conjunctivitis (Fig. 6). It was thus of interest to compare the traits of ECC strains isolated from conjunctivitis to those isolated from the nasopharynx by investigating the presence or absence of a selection of newly identified ECC genes with a putative contribution to conjunctivitis pathogenesis. From the asymptomatic carriage data sets, we selected genome sequences of 96 strains that were of sequence types closely related to those that constituted the ECC group, and also diverse strains spread across the phylogenetic tree representing the most prevalent STs associated with nasopharyngeal carriage regardless of their encapsulation status (Fig. 6, Supplementary Fig. 7 and

Supplementary Data 7). All genes found to be enriched in ECC strains isolated from conjunctivitis were also found to be present within nasopharyngeal isolates of ST448, ST2315 and ST344 genomes, indicating that these strains are highly similar to those isolated from conjunctivitis, and supporting an infection model where asymptomatic carriage in the nasopharynx precedes ocular infection. Of the cumulative 3,701 nasopharyngeal isolates represented in the two nasopharyngeal surveys, no representatives of ST1186 or ST1270 were observed, in contrast to their occurrence at rates of 13/271 (4.8%) and 3/271 (1.1%), respectively, in conjunctivitis cases, indicating their rarity among the circulating population despite their enrichment in cases of conjunctivitis.

Genes we identified as enriched in ECC strains isolated from conjunctivitis, *cbpAC1*, *cbpAC2* and *nanO1/nanO2*, were only found to occur among asymptomatic carriage strains of the same sequence types. Other genes that we found to be enriched in ECC (*sspBC1*, *sspBC2*, *zmpC1* and *zmpC2*) also occurred in unencapsulated lineages that have not yet been observed in conjunctivitis, and the majority of these lineages are closely related phylogenetically to ECC strains (Fig. 6). Interestingly, some sequence types phylogenetically closely related to ECC strains (ST5126, ST4142 and ST4139) were found to lack all ECC genes that were investigated. As these STs were not identified among conjunctivitis strains, their ability to cause this disease remains unknown.

### Discussion

With a view towards understanding strain diversity and the molecular basis for virulence of *S. pneumoniae* in conjunctivitis, and to improving vaccine design to cover this disease, we characterized recent isolates from across the United States. We found that nearly 90% of conjunctivitis cases were caused by five related STs (ST448, ST344, ST1186, ST1270 and ST2315) that occur within a distinct cluster of the *S. pneumoniae* species (see Fig. 6 and Supplementary Fig. 7), a population structure supported by two recent reports<sup>19,41</sup>. This divergence is characterized by novel gene content constituting ~10% of the genome. Although ECC strains possess a large amount of novel genes, shared genes exhibit an ANI of  $97.9\% \pm 0.11$  ANI with strains from other types of infection, and therefore ECC

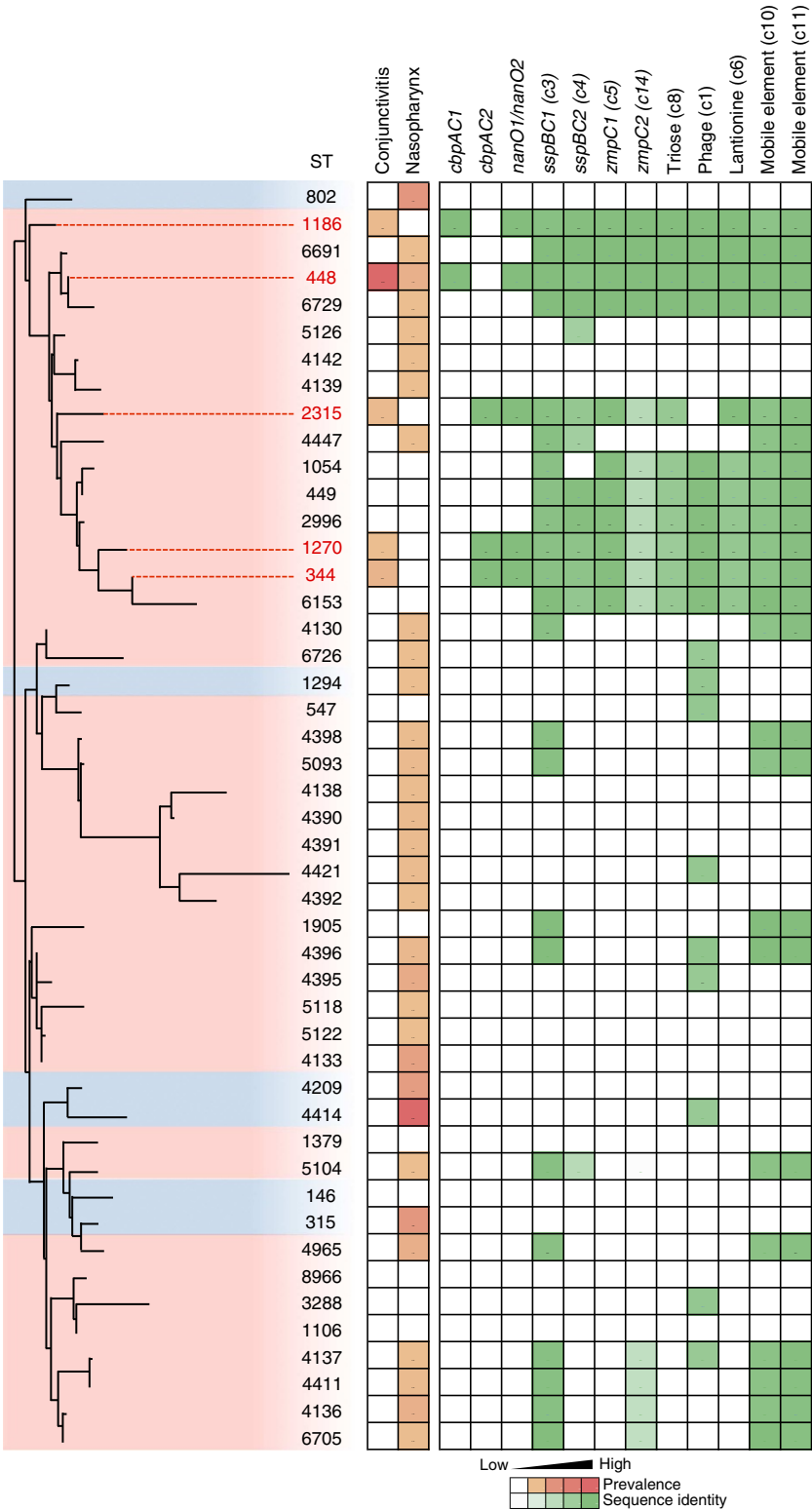


**Figure 6 | Presence of ECC genes in genomes of nasopharyngeal isolates.** All STs representative of unencapsulated strains (pink highlight), and the most prevalent encapsulated strains (blue highlight), from two recent large-scale surveys of asymptomatic nasopharyngeal carriage<sup>19,41</sup>, compared with ECC members associated with conjunctivitis (red text and line extension), shown in a PhyML SNP-based tree based on the concatenated alignments of MLST alleles. Bootstrapping was performed with 1,000 iterations. Prevalence in conjunctivitis (this study) and nasopharyngeal carriage<sup>41</sup> is shown. Percent presence and sequence identity of gene (*gene*, cluster number) or cluster (predicted function, cluster number) is denoted with green boxes.

strains do not constitute a new species (ANI < 95%) by this definition<sup>19,21,42</sup>. We found that genes *cbpAC1*, *cbpAC2*, *nanO1* and *nanO2* were only carried by STs that are associated with conjunctivitis (see

Figs 6 and 7). Other genes enriched in ECC, including the *sspBC* agglutinins, *zmpC1*, *zmpC2* and the triose metabolic cassette, were found to be shared among a few closely related unencapsulated STs (ST6153, ST6691, ST6729, ST2996, ST1054 and ST449) that

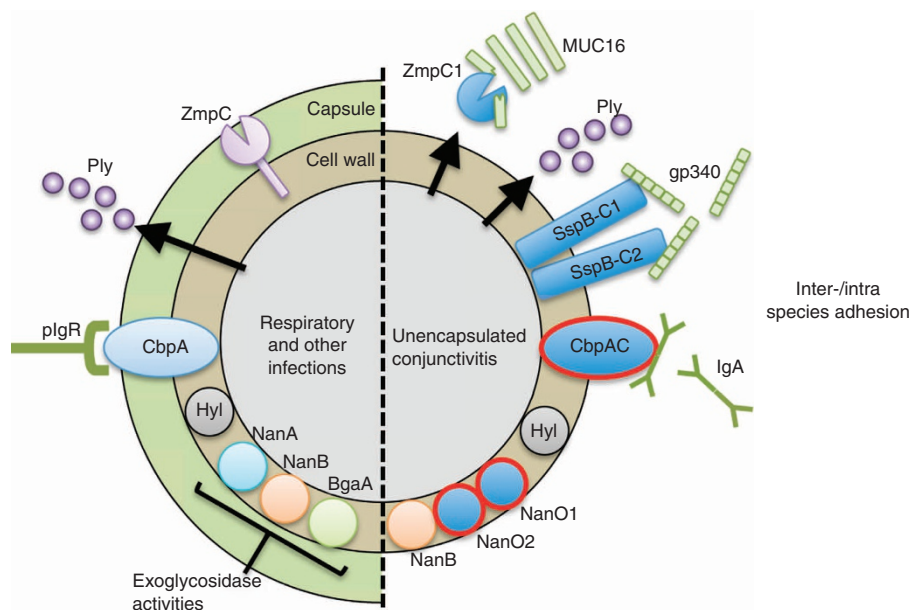


**Figure 7 | Virulence factor differences between invasive and ECC strains.** New traits found within ECC and closely related genomes are shown in solid blue, with those unique to STs associated with conjunctivitis highlighted with red outline. CbpAC1 and CbpAC2 are shown as CbpAC, since ECC strains express one or the other, but not both. Predicted ligands for SspBC1, SspBC2 and CbpAC are shown. Host-derived molecules are illustrated in green. Arrows indicate secreted products.

have not been identified in cases of conjunctivitis, which may stem from the paucity of studies that have identified MLST types of *S. pneumoniae* causing conjunctivitis. These additional genes are largely absent in encapsulated and more distantly related unencapsulated genomes unrelated to conjunctivitis however (see Figs 6 and 7). These findings suggest that some of the genes enriched in ECC are fundamental to the formation of the larger unencapsulated lineage to which ECC members belong (see Fig. 6 and Supplementary Fig. 7).

Typifying the conjunctivitis-associated strains is a lack of capsule, rendering them unaffected by current polyvalent pneumococcal capsule vaccines. As would be predicted for a lineage that professionally lacks the polyanionic capsule through which surface proteins must fold and extend, these strains have substantially different surface features, including those known to contribute to virulence (Fig. 7). Novel features, specific to ECC STs include substantially altered forms of CbpA, CbpAC1 and CbpAC2. Interestingly, these no longer possess the key domain that mediates binding to host polymeric Ig receptor, which *S. pneumoniae* use to facilitate transcytosis from nasopharyngeal epithelia into the blood stream<sup>35</sup>. Instead, both CbpAC1 and CbpAC2 appear to have independently swapped that domain for one that mediates direct binding to secretory IgA<sup>33,36,43</sup>. The implication is that ECC strains bind secretory IgA in a subtly, but importantly, different way, possibly coating themselves with IgA, in a manner analogous to that mediated by protein A of *S. aureus*<sup>44</sup>. Alternatively, these CbpA variants may act as adhesins for attachment to surfaces coated with antibodies, as suggested for immunoglobulin receptors in *S. pyogenes*<sup>45</sup>. That this change appears to have occurred twice, and that only variants of CbpA occur in unencapsulated STs associated with conjunctivitis, suggests that it is important for the ocular tropism. In addition to the variant CbpA, all ECC genomes also encode two novel, divergent choline-binding protein CbpI's, here termed CbpI1 and CbpI2. No function has yet been ascribed to CbpI, CbpI1 or CbpI2.

Other factors unique to STs associated with conjunctivitis that could affect the host/microbe interface include the displacement of NanA with two variant sialidases, NanO1 and NanO2. This

recombination event is seen only in ECC members and is absent even in the closest non-ECC relatives. Since sialic acid residues exhibit variation among host cell types, it has been suggested that they are mediators of tissue tropism<sup>46</sup>. This is of potential relevance to conjunctivitis, since proteins found at the ocular surface are decorated by covalently bound sialic acids<sup>47</sup>, which have been shown to mediate ocular surface binding of *Pseudomonas aeruginosa* and *Escherichia coli*<sup>48,49</sup>.

A recurring motif was the replacement of surface features optimized for function in the presence of a capsule, with surface features derived from unencapsulated oral streptococci (for example, *S. mitis*). Others have noted that *S. mitis* appears to be a reservoir of genetic diversity<sup>50</sup>. Additional novel surface features of ECC and closely related unencapsulated strains likely involved in colonization, and likely originating in oral streptococci, include two Antigen I/II (Agl/II) family of adhesins/agglutinins encoded in separate genomic islands, SspBC1 and SspBC2. Notably, *sspBC2* is restricted to ECC and closely related strains potentially implicating its involvement in the unusual ocular surface tropism, whereas *sspBC1* is also found within more distantly unencapsulated genomes, implicating its possible involvement in colonization of the nasopharynx and adnexa (see Fig. 6). The Agl/II family of adhesins is central to colonization and biofilm formation by commensal and pathogenic species of *Streptococcus*<sup>24,51</sup>. A previous review noted their ubiquitous presence among streptococci except for *S. pneumoniae*<sup>51</sup>. The observation here that these genes occur in unencapsulated strains of *S. pneumoniae* suggests either incompatibility or functional redundancy with the pneumococcal capsule. In terms of colonization (nasopharyngeal and/or ocular) and conjunctivitis pathogenesis, SspB domains of Agl/II proteins mediate binding to human scavenger protein gp-340 (ref. 24), which occurs in tears and on the ocular surface<sup>52</sup>.

All STs associated with conjunctivitis encoded a novel phage element (cluster 9/cluster 11). This element was also seen in closely related unencapsulated nasopharyngeal strains, whereas it was rarely found in more distantly related unencapsulated strains. Interestingly, this element is located at different sites in the genomes of the conjunctivitis-associated sequence types but is

always consistent within an ST. This suggests that it was lacking from a common ancestor and has been acquired independently, or that it is internally mobile. There are no obvious adhesins or virulence traits encoded within this element; however, it may contribute to biofilm formation as described for other phage elements in *S. pneumoniae*<sup>53</sup>. Its presence within numerous nasopharyngeal STs suggests that it may play a basic function in colonization for unencapsulated varieties of *S. pneumoniae*.

A unique metabolic feature profile was found among ECC and closely related strains, suggesting that their colonization ability is likely nutritionally distinct from that of strains associated with invasive infection. A phosphoenolpyruvate-dihydroxyacetone PTS gene cluster occurring in ECC and closely related nasopharyngeal strains and only one distantly related strain from otitis media (Hungary19A-6, cluster 8), also found in *S. mitis* and *S. pseudopneumoniae*, suggests that the ability to metabolize Dha is important for mucosal surface colonization. DhaP was detected among the phosphorylated intermediate metabolites present on the ocular sclera and corneal tissues<sup>54</sup>.

In addition to the gain of putative metabolic capabilities described above, all ST genomes associated with conjunctivitis lacked the ability to metabolize fucose, a sugar that decorates ocular glycans present in the glycocalyx of corneal epithelial cells<sup>49</sup>. Fucosylated glycans coating mucins are known to promote bacterial colonization in the gut, serving as both adherence targets, as well as a carbon source<sup>55,56</sup>. Specifically at the ocular surface, fucose residues have been implicated in the attachment of *P. aeruginosa* and *E. coli* to ocular epithelial cells<sup>49</sup>. Moreover, application of exogenous fucose was shown to suppress inflammation in rabbit corneal and explanted human cornea models of wound-healing<sup>57</sup>. Nasopharyngeal STs closely related to ECC members (ST6691, ST6729, ST1054, ST449, ST2996 and ST6153) were also found to lack the elements to metabolize fucose. These findings suggest that the inability to metabolize fucose is irrelevant for colonizing the nasopharynx but may confer an advantage at the ocular surface, potentially by promoting an anti-inflammatory environment and/or by preserving an important bacterial ligand.

While asymptomatic carriage in the nasopharyngeal cavity is likely to be a precursor to infection, ST448 (refs 9,12,13,15,18) and related STs commonly isolated conjunctivitis were not highly prevalent in recent large-scale surveys of asymptomatic *S. pneumoniae* carriage in the nasopharynx<sup>19,41</sup>. Whereas ST448 was found to be by far the leading cause of conjunctivitis in this study as well as in others<sup>15,18</sup>, it represented only 1.43% of 3,084 isolates found to be asymptotically carried by Chewapreecha *et al.*<sup>41</sup>, and 1.14% of nasopharyngeal isolates examined by Croucher *et al.*<sup>19</sup> Indeed, there are four other unencapsulated STs found at similar or higher prevalence within the nasopharynxes (ST4133, ST4395, ST4965 and ST4136 ranging from 1.43 to 2.92%), the most prevalent of which, ST4133, has not been reported as a cause of conjunctivitis, is not closely related to the STs most commonly associated with conjunctivitis and does not encode the genes enriched in ECC that were searched, highlighting the point that it is not the simple lack of capsule that predisposes these strains to cause conjunctivitis. The four most common STs (ST4414, ST802, ST315 and ST4209) in nasopharyngeal carriage are all encapsulated (a cumulative 19.98% of 3,084 isolates), and lack all ECC-associated genes (except for a phage (cluster 1) shared only in ST4414) and were not found among our collection of 271 conjunctivitis isolates. Similar findings were seen by Croucher *et al.*<sup>19</sup>, with 1.14% of nasopharyngeal isolates being ST448 (21st most common ST), in this case representing the most common unencapsulated ST recovered in their study. Taken together, these findings highlight that prevalence in the nasopharynxes does not directly correlate with conjunctival infection, in further support of

the hypothesis that genes unique to ECC genomes are critical for conjunctival infection.

It is unlikely that the unencapsulated cluster containing ECC members arose because of vaccine use, as has been speculated<sup>8</sup>, based on the extent of divergence between ECC lineages investigated herein and non-ocular lineages (an average  $27,754 \pm 1,831$  SNPs). On the basis of a recent determination of *S. pneumoniae* mutation rate<sup>58</sup> (and assuming that this measure is true for ECC members as well), the bifurcation between ECC and the main branch of the species took place  $\sim 8,400$  years ago ( $8,385 \pm 553$  years). That the rate of divergence measured for other *S. pneumoniae* also applies to ECC rates of change stems from a comparison of the distance between strains isolated from geographically and temporally related outbreaks in Maine and New Hampshire. With epidemiologic centers about 7 months apart, strains from the New Hampshire outbreak (ECC\_1854 and ECC\_1910) differ from those from the Maine outbreak (ECC\_0072 and ECC\_0083)  $4.67 \pm 2.1$  SNPs, a mutation rate of  $1.43 \times 10^{-6}$  substitutions per site per year, in agreement with previous calculations  $1.57 \times 10^{-6}$  substitutions per site per year<sup>58</sup>. This dating is similar to estimates of clade divergence in *E. faecium*<sup>59</sup> and *S. aureus*<sup>60</sup> both of which were attributed to increasing urbanization. This suggests that, in contrast to the ancestral line, there is an especially important role for person-to-person transmission in the propagation of either this lineage or the branch associated with respiratory infection.

In summary, we found that five STs commonly associated with conjunctivitis (which accounted for 90% of *S. pneumoniae* conjunctivitis cases studied) belong to a distinct cluster of unencapsulated strains within the *S. pneumoniae* species. These strains are typified by substantially different features including elements exclusive to strains associated with conjunctivitis (CbpAC1, CbpAC2, NanO1 and NanO2) that may contribute to their ocular tropism. Additional features were shared with only closely related unencapsulated varieties (for example, ZmpC and SspBC2) or sporadically among distantly related unencapsulated strains (for example, SspBC1). Currently, 90% of the *S. pneumoniae* strains associated with conjunctivitis are not covered by existing vaccines. Furthermore, because of the extensive variation observed, vaccines under development that target conventional *S. pneumoniae* virulence traits (for example, CbpA) may or may not provide coverage for preventing conjunctivitis. This knowledge of conserved and variant features occurring in the ECC members will be critical for future vaccine-design strategies.

## Methods

**Bacterial strains.** A large and comprehensive collection of 280 *S. pneumoniae* conjunctivitis strains were assembled from across the United States of America, including 271 isolates obtained from 72 different zip codes, as well as one isolate from New Delhi, India as part of a national, multicentre, passive surveillance study of bacterial conjunctivitis<sup>5-7</sup>. In addition, included were two conjunctivitis isolates (six in total) from each large outbreak occurring at Dartmouth College<sup>10,12</sup>, an elementary school in Maine<sup>13,17</sup>, and a suburb of Minnesota<sup>9</sup>, as well as three other conjunctivitis isolates of unknown origin were obtained from the CDC Streptococcus Laboratory (Supplementary Data 1). Strains were cultured on 5% sheep blood agar plates (BD Biosciences, San Jose, CA) or in Todd Hewitt broth supplemented with 5% yeast extract, and incubated at 37 °C in 5% CO<sub>2</sub>. Bacterial isolates were confirmed as *S. pneumoniae* based on their haemolysis phenotype on blood agar plates, bile solubility and susceptibility to optochin when grown in a 5% CO<sub>2</sub> atmosphere<sup>8</sup>.

**Ocular isolate characterization by MLST and capsule typing.** Multilocus sequence typing and capsule typing were performed on the 271 strains collected from the large US multicentre trial<sup>5-7</sup> (Fig. 1b). Briefly, sequence types were determined based on sequences for *aroE*, *gdh*, *gki*, *recP*, *spi*, *xpt* and *ddl* genes<sup>61</sup>. The presence of capsule was determined with both OMNI serum, as well as the capsule-type-specific Pneumotest-Latex serum, both obtained from the Statens Serum Institut (MiraVista Diagnostics, Indianapolis, IN). Initial capsule typing

resulting for 50 selected isolates were confirmed by the Statens Serum Institut in Denmark. A preliminary report of the distribution of MLST types has been presented previously<sup>62</sup>.

**Genome sequencing.** Strains isolated from three well-documented major US outbreaks in Maine, New Hampshire and Minnesota, as well as strains that were representative of the MLST sequence types most prevalent among the 271 strains collected from the multicentre US study, were selected for genome sequencing (Supplementary Data 1). Briefly, total DNA was purified from a 5-ml overnight culture using the DNeasy DNA extraction kit (Qiagen, Valencia, CA). Library preparation for Illumina sequencing by Illumina was carried out using the Nextera DNA Sample Preparation kit (Illumina, San Diego, CA), according to the manufacturer's specifications. DNA quality was verified on a Bio-Tek Synergy 2 microplate reader (Winooski, VT) before quantification using a Qubit fluorometer and dsDNA High-Sensitivity assay kit (Invitrogen, Carlsbad, CA). A transposome was used to simultaneously fragment and append adapter sequences to 50 ng of DNA per sample, followed by addition of dual-index sequences in a limited-cycle PCR step. Quality and quantity of each sample library was measured on an Agilent Technologies 2100 Bioanalyzer (Santa Clara, CA), with a target fragment size of ~300 bp. The genomes of strains ECC\_0072, ECC\_0083, ECC\_1854, ECC\_1910, SC\_0381 and SC\_0391 were sequenced at the St Jude Children's Hospital Hartwell Center for Bioinformatics and Biotechnology, Memphis, TN on an Illumina GAXII sequencer, according to the manufacturer's specifications. For all other genomes, libraries were normalized to 2 nM, multiplexed and subjected to either 150, 200 or 250 bp paired end sequencing on an Illumina MiSeq Personal Sequencer at the Mass Eye and Ear Infirmary Ocular Genomics Institute (Boston, MA), according to the manufacturer's specifications.

**Genome assemblies and annotation.** Sequence reads were assembled *de novo* utilizing CLC Genomics Workbench v4.9 (CLC Bio, Cambridge, MA; Supplementary Data 3). On average, 3.7 million high-quality paired-end reads were collected for each strain, representing >240-fold coverage of the ~2.1-Mb genomes. Sequence reads below a quality score of 25 at any position were excluded from further analyses. All genomes compared in this study (Supplementary Data 2) were annotated using the Rapid Annotation using Subsystem Technology (RAST) server<sup>63</sup>, and Glimmer v.3 (ref. 64), with comparison to family profiles in the FIGfam (protein families generated by the Fellowship for Interpretation of Genomes) release 63 database. Wherever possible, manual search of the PFAM<sup>65</sup> database was used to assign functions to genes annotated as hypothetical.

**Orthogroups and gene families.** Orthogroups were calculated across all of the genomes in our data set using OrthoMC<sup>66</sup>, with a BLAST *e*-value of  $10^{-5}$  and an inflation index of 2.5. Orthogroups contain orthologues, which are vertically inherited genes that likely have the same function, and also possibly paralogues, which are duplicated genes that may have different functions.

**Phylogenic and ANI analyses.** SNP-based phylogeny based on MLST allele sequence and single-copy core alignment was generated using PhyML and statistics were calculated for 1,000 bootstrap replicates<sup>67</sup>. To generate a MLST-based tree, DNA sequences for the seven MLST loci were concatenated and aligned for each of the 31 sequence types represented in the conjunctivitis isolates (Fig. 2) and the 26 non-ocular reference genomes (Supplementary Data 2).

A phylogenetic tree of all genomes in our data set, including the 21 genomes newly sequenced as well as 26 reference genomes (Supplementary Data 2), was generated using all 1,160 single-copy core orthogroups, including *S. mitis* strain B6 as an outgroup. The BRAT NextGen analysis was conducted on the 1,160 single-copy core orthogroup alignment of the 47 *S. pneumoniae* genomes to identify the filtered-out recombinogenic regions<sup>19,68</sup>. Percent ANI was calculated by dividing the number of identical nucleotide residues in shared genes by the total number of nucleotides in shared genes<sup>21</sup>. Shared gene content between strains in pairwise genome comparisons was generated by searching the CDS predictions from one genome annotation against the annotations of the second genome and conserved genes were identified by BLAST matching >60% overall sequence identity<sup>21</sup>.

**Identification of antibiotic resistance genes.** The Resfinder database was used to identify candidate antibiotic resistance genes as described previously<sup>69</sup>. For a subset of the isolates, susceptibility was tested in microtitre plates and minimum inhibitory concentrations were determined by broth microdilution according to the procedure recommended by the Clinical and Laboratory Standards Institute.

**Western blot.** Logarithmically growing cells (optical density (OD)<sub>600</sub> = 0.5) were pelleted with centrifugation and subjected to lysis in 0.1% Triton X-100. To ensure equal loading, protein concentration was determined for each lysate via absorbance at 280 nm and loaded accordingly. Duplicate gels stained with Coomassie were used to confirm equivalent loading. Lysates were run on 10% NuPAGE Bis-Tris gels (Invitrogen). Proteins were subsequently transferred to polyvinylidene fluoride membranes using western blot analysis. CbpA was detected using three

monoclonal antibodies (1:5,000) in PBS-T/5% non-fat dry milk. The three monoclonal antibodies (14A3, 3G12 and 3H11) recognize the highly conserved loop regions in the R2 domain of CbpA and were generated as previously described<sup>34</sup>. Pneumolysin was detected using rabbit polyclonal serum generated against recombinant pneumolysin. Secondary horseradish peroxidase (HRP)-conjugated antibodies (Bio-Rad, Hercules, CA) were used at 1:5,000 in PBS-T/5% non-fat dry milk. Images of the complete western blots are provided in Supplementary Fig. 8.

**Aggregation assays with gp-340.** Bacterial isolates (ST448, ECC\_3540 and ST199, SC\_3526) were cultured overnight in Todd Hewitt broth, pelleted after centrifugation (5,000 × *g* for 10 min), washed twice in PBS and resuspended to an OD at OD<sub>600</sub> = 0.6 in PBS. Bacterial suspensions (300 µl) were incubated in 5 ml culture tubes in an orbital shaker at 300 r.p.m. for 1 h at 37 °C with 0, 0.5 and 1.0 µg ml<sup>-1</sup> of purified gp-340 (DMBT-1 recombinant human protein, Life Technologies). Tubes were then rested for 1 h at 37 °C to allow bacterial aggregates to settle. Gram staining was performed for each reaction to demonstrate bacterial aggregation and representative images were acquired using an Olympus BX60 microscope.

**Characterization of ECC genes in nasopharyngeal genomes.** Additional genomes of nasopharyngeal isolates were analysed for genes found in our original data set to be specific to ECC genomes including: (a) 29 additional representatives of strains known to be associated with ECC (23 ST448, 4 SLV448, 1 ST344 and 1 ST2315), (b) 19 representatives of STs closely related to those associated with ECC, (c) 44 unencapsulated STs not closely related to ECC members were analysed (Supplementary Data 7), (d) 4 encapsulated STs that were most prevalent in Chewapreecha *et al.*<sup>41</sup> This included all unencapsulated nasopharyngeal genomes in Croucher *et al.*<sup>19</sup> (16 genomes) and eight draft genomes of nasopharyngeal isolates currently available from either the NCBI GenBank or European Nucleotide Archive, including five genomes newly deposited to NCBI GenBank<sup>70</sup>. When available, we maximized the diversity of this set by downloading several representatives, spanning various dates of isolation, or when additional information on strain diversity was available (for example, Bayesian Analysis of Population Structure<sup>41</sup>). Genomes were downloaded from the European Nucleotide Archive read archive and assembled using CLC Genomics Workbench as described above. All together, an additional 96 genomes of nasopharyngeal origin were selected to serve as a local BLAST database, which was used to search (>80% query coverage, >80% nucleotide identity) for the presence of genes identified as specific to the ECC genes in our original data set (Supplementary Data 7).

## References

1. Tuomanen, E. I., Austrian, R. & Masure, H. R. Pathogenesis of pneumococcal infection. *N. Engl. J. Med.* **332**, 1280–1284 (1995).
2. Vernatter, J. & Pirofski, L. A. Current concepts in host-microbe interaction leading to pneumococcal pneumonia. *Curr. Opin. Infect. Dis.* **26**, 277–283 (2013).
3. Farrell, D. J., Klugman, K. P. & Pichichero, M. Increased antimicrobial resistance among nonvaccine serotypes of *Streptococcus pneumoniae* in the pediatric population after the introduction of 7-valent pneumococcal vaccine in the United States. *Pediatr. Infect. Dis. J.* **26**, 123–128 (2007).
4. Buznach, N., Dagan, R. & Greenberg, D. Clinical and bacterial characteristics of acute bacterial conjunctivitis in children in the antibiotic resistance era. *Pediatr. Infect. Dis. J.* **24**, 823–828 (2005).
5. Karpecki, P. *et al.* Besifloxacin ophthalmic suspension 0.6% in patients with bacterial conjunctivitis: A multicenter, prospective, randomized, double-masked, vehicle-controlled, 5-day efficacy and safety study. *Clin. Ther.* **31**, 514–526 (2009).
6. McDonald, M. B. *et al.* Efficacy and safety of besifloxacin ophthalmic suspension 0.6% compared with moxifloxacin ophthalmic solution 0.5% for treating bacterial conjunctivitis. *Ophthalmology* **116**, 1615–1623 (2009).
7. Tepedino, M. E. *et al.* Phase III efficacy and safety study of besifloxacin ophthalmic suspension 0.6% in the treatment of bacterial conjunctivitis. *Curr. Med. Res. Opin.* **25**, 1159–1169 (2009).
8. Haas, W., Hesje, C. K., Sanfilippo, C. M. & Morris, T. W. High proportion of nontypeable *Streptococcus pneumoniae* isolates among sporadic, nonoutbreak cases of bacterial conjunctivitis. *Curr. Eye Res.* **36**, 1078–1085 (2011).
9. Buck, J. M. *et al.* A community outbreak of conjunctivitis caused by nontypeable *Streptococcus pneumoniae* in Minnesota. *Pediatr. Infect. Dis. J.* **25**, 906–911 (2006).
10. Martin, M. *et al.* An outbreak of conjunctivitis due to atypical *Streptococcus pneumoniae*. *N. Engl. J. Med.* **348**, 1112–1121 (2003).
11. Shayegani, M., Parsons, L. M., Gibbons, Jr. W. E. & Campbell, D. Characterization of nontypeable *Streptococcus pneumoniae*-like organisms isolated from outbreaks of conjunctivitis. *J. Clin. Microbiol.* **16**, 8–14 (1982).

12. Centers for Disease Control and Prevention (CDC). Outbreak of bacterial conjunctivitis at a college--New Hampshire, January-March, 2002. *Morb. Mortal. Wkly Rep.* **51**, 205–207 (2002).
13. Centers for Disease Control and Prevention (CDC). Pneumococcal conjunctivitis at an elementary school--Maine, September 20–December 6, 2002. *Morb. Mortal. Wkly Rep.* **52**, 64–66 (2003).
14. Crum, N. F., Barrozo, C. P., Chapman, F. A., Ryan, M. A. & Russell, K. L. An outbreak of conjunctivitis due to a novel unencapsulated *Streptococcus pneumoniae* among military trainees. *Clin. Infect. Dis.* **39**, 1148–1154 (2004).
15. Hanage, W. P., Kaijalainen, T., Saukkoriipi, A., Rickcord, J. L. & Spratt, B. G. A successful, diverse disease-associated lineage of nontypeable pneumococci that has lost the capsular biosynthesis locus. *J. Clin. Microbiol.* **44**, 743–749 (2006).
16. Enright, M. C. & Spratt, B. G. A multilocus sequence typing scheme for *Streptococcus pneumoniae*: identification of clones associated with serious invasive disease. *Microbiology* **144** (Pt 11), 3049–3060 (1998).
17. Zegans, M. E. *et al.* Clinical features, outcomes, and costs of a conjunctivitis outbreak caused by the ST448 strain of *Streptococcus pneumoniae*. *Cornea* **28**, 503–509 (2009).
18. Marimon, J. M., Ercibengoa, M., Garcia-Arenzana, J. M., Alonso, M. & Perez-Trallero, E. *Streptococcus pneumoniae* ocular infections, prominent role of unencapsulated isolates in conjunctivitis. *Clin. Microbiol. Infect.* **19**, E298–E305 (2013).
19. Croucher, N. J. *et al.* Population genomics of post-vaccine changes in pneumococcal epidemiology. *Nat. Genet.* **45**, 656–663 (2013).
20. Marttinen, P. *et al.* Detection of recombination events in bacterial genomes from large population samples. *Nucleic Acids Res.* **40**, e6 (2012).
21. Konstantinidis, K. T. & Tiedje, J. M. Genomic insights that advance the species definition for prokaryotes. *Proc. Natl Acad. Sci. USA* **102**, 2567–2572 (2005).
22. Keller, L. E. *et al.* PspK of *Streptococcus pneumoniae* increases adherence to epithelial cells and enhances nasopharyngeal colonization. *Infect. Immun.* **81**, 173–181 (2013).
23. Park, I. H. *et al.* Nontypeable pneumococci can be divided into multiple cps types, including one type expressing the novel gene pspK. *MBio* **3**, pii: e00035-12 (2012).
24. Jakubovics, N. S., Stromberg, N., van Dolleweerd, C. J., Kelly, C. G. & Jenkinson, H. F. Differential binding specificities of oral streptococcal antigen I/II family adhesins for human or bacterial ligands. *Mol. Microbiol.* **55**, 1591–1605 (2005).
25. Govindarajan, B. *et al.* A metalloproteinase secreted by *Streptococcus pneumoniae* removes membrane mucin MUC16 from the epithelial glycocalyx barrier. *PLoS ONE* **7**, e32418 (2012).
26. Menon, B. B. & Govindarajan, B. Identification of an atypical zinc metalloproteinase, ZmpC, from an epidemic conjunctivitis-causing strain of *Streptococcus pneumoniae*. *Microb. Pathog.* **56**, 40–46 (2013).
27. Pettigrew, M. M., Fennie, K. P., York, M. P., Daniels, J. & Ghaffar, F. Variation in the presence of neuraminidase genes among *Streptococcus pneumoniae* isolates with identical sequence types. *Infect. Immun.* **74**, 3360–3365 (2006).
28. Gosink, K. K., Mann, E. R., Guglielmo, C., Tuomanen, E. I. & Masure, H. R. Role of novel choline binding proteins in virulence of *Streptococcus pneumoniae*. *Infect. Immun.* **68**, 5690–5695 (2000).
29. Bagnoli, F. *et al.* A second pilus type in *Streptococcus pneumoniae* is prevalent in emerging serotypes and mediates adhesion to host cells. *J. Bacteriol.* **190**, 5480–5492 (2008).
30. Hillerlingmann, M. *et al.* Molecular architecture of *Streptococcus pneumoniae* TIGR4 pili. *EMBO J.* **28**, 3921–3930 (2009).
31. Mook-Kanamori, B. B., Geldhoff, M., van der Poll, T. & van de Beek, D. Pathogenesis and pathophysiology of pneumococcal meningitis. *Clin. Microbiol. Rev.* **24**, 557–591 (2011).
32. Luo, R. *et al.* Solution structure of choline binding protein A, the major adhesin of *Streptococcus pneumoniae*. *EMBO J.* **24**, 34–43 (2005).
33. Jerlstrom, P. G., Chhatwal, G. S. & Timmis, K. N. The IgA-binding beta antigen of the c protein complex of Group B streptococci: sequence determination of its gene and detection of two binding regions. *Mol. Microbiol.* **5**, 843–849 (1991).
34. Mann, B. *et al.* Broadly protective protein-based pneumococcal vaccine composed of pneumolysin toxoid-CbpA peptide recombinant fusion protein. *J. Infect. Dis.* **209**, 1116–1125 (2014).
35. Zhang, J. R. *et al.* The polymeric immunoglobulin receptor translocates pneumococci across human nasopharyngeal epithelial cells. *Cell* **102**, 827–837 (2000).
36. Jerlstrom, P. G., Talay, S. R., Valentin-Weigand, P., Timmis, K. N. & Chhatwal, G. S. Identification of an immunoglobulin A binding motif located in the beta-antigen of the c protein complex of group B streptococci. *Infect. Immun.* **64**, 2787–2793 (1996).
37. Rosch, J. W., Mann, B., Thornton, J., Sublett, J. & Tuomanen, E. Convergence of regulatory networks on the pilus locus of *Streptococcus pneumoniae*. *Infect. Immun.* **76**, 3187–3196 (2008).
38. Brown, J. S., Gilliland, S. M., Spratt, B. G. & Holden, D. W. A locus contained within a variable region of pneumococcal pathogenicity island 1 contributes to virulence in mice. *Infect. Immun.* **72**, 1587–1593 (2004).
39. Frost, L. S., Leplae, R., Summers, A. O. & Toussaint, A. Mobile genetic elements: the agents of open source evolution. *Nat. Rev. Microbiol.* **3**, 722–732 (2005).
40. Haas, W., Gearing, L. S., Hesje, C. K., Sanfilippo, C. M. & Morris, T. W. Microbiological etiology and susceptibility of bacterial conjunctivitis isolates from clinical trials with ophthalmic, twice-daily besifloxacin. *Adv. Ther.* **29**, 442–455 (2012).
41. Chewapreecha, C. *et al.* Dense genomic sampling identifies highways of pneumococcal recombination. *Nat. Genet.* **46**, 305–309 (2014).
42. Konstantinidis, K. T., Ramette, A. & Tiedje, J. M. The bacterial species definition in the genomic era. *Philos. Trans. R. Soc. Lond. B. Biol. Sci.* **361**, 1929–1940 (2006).
43. Michel, J. L., Madoff, L. C., Kling, D. E., Kasper, D. L. & Ausubel, F. M. Cloned alpha and beta C-protein antigens of group B streptococci elicit protective immunity. *Infect. Immun.* **59**, 2023–2028 (1991).
44. Kim, H. K., Thammavongsa, V., Schneewind, O. & Missiakas, D. Recurrent infections and immune evasion strategies of *Staphylococcus aureus*. *Curr. Opin. Microbiol.* **15**, 92–99 (2012).
45. Fagan, P. K., Reinscheid, D., Gottschalk, B. & Chhatwal, G. S. Identification and characterization of a novel secreted immunoglobulin binding protein from group A streptococcus. *Infect. Immun.* **69**, 4851–4857 (2001).
46. Lofling, J., Vimberg, V., Battig, P. & Henriques-Normark, B. Cellular interactions by LPxTG-anchored pneumococcal adhesins and their streptococcal homologues. *Cell. Microbiol.* **13**, 186–197 (2011).
47. Wells, P. A. & Hazlett, L. D. Complex carbohydrates at the ocular surface of the mouse: an ultrastructural and cytochemical analysis. *Exp. Eye Res.* **39**, 19–35 (1984).
48. Hazlett, L. D., Moon, M. & Berk, R. S. *In vivo* identification of sialic acid as the ocular receptor for *Pseudomonas aeruginosa*. *Infect. Immun.* **51**, 687–689 (1986).
49. Royle, L. *et al.* Glycan structures of ocular surface mucins in man, rabbit and dog display species differences. *Glycoconj. J.* **25**, 763–773 (2008).
50. Donati, C. *et al.* Structure and dynamics of the pan-genome of *Streptococcus pneumoniae* and closely related species. *Genome Biol.* **11**, R107 (2010).
51. Brady, L. J. *et al.* The changing faces of Streptococcus antigen I/II polypeptide family adhesins. *Mol. Microbiol.* **77**, 276–286 (2010).
52. Jumblatt, M. M. *et al.* Glycoprotein 340 in normal human ocular surface tissues and tear film. *Infect. Immun.* **74**, 4058–4063 (2006).
53. Carrolo, M., Frias, M. J., Pinto, F. R., Melo-Cristino, J. & Ramirez, M. Prophage spontaneous activation promotes DNA release enhancing biofilm formation in *Streptococcus pneumoniae*. *PLoS ONE* **5**, e15678 (2010).
54. Sachedina, S., Greiner, J. V. & Glonek, T. Phosphatic intermediate metabolites of the porcine ocular tunica fibrosa. *Exp. Eye Res.* **52**, 253–260 (1991).
55. Pacheco, A. R. *et al.* Fucose sensing regulates bacterial intestinal colonization. *Nature* **492**, 113–117 (2012).
56. Stahl, M. *et al.* L-fucose utilization provides *Campylobacter jejuni* with a competitive advantage. *Proc. Natl Acad. Sci. USA* **108**, 7194–7199 (2011).
57. Isnard, N., Boursles-Dagonet, F., Robert, L. & Renard, G. Studies on corneal wound healing. Effect of fucose on iodine vapor-burnt rabbit corneas. *Ophthalmologica* **219**, 324–333 (2005).
58. Croucher, N. J. *et al.* Rapid pneumococcal evolution in response to clinical interventions. *Science* **331**, 430–434 (2011).
59. Lebreton, F. *et al.* Emergence of epidemic multidrug-resistant *Enterococcus faecium* from animal and commensal strains. *MBio* **4**, pii: e00534-13 (2013).
60. Weinert, L. A. *et al.* Molecular dating of human-to-bovid host jumps by *Staphylococcus aureus* reveals an association with the spread of domestication. *Biol. Lett.* **8**, 829–832 (2012).
61. Maiden, M. C. *et al.* Multilocus sequence typing: a portable approach to the identification of clones within populations of pathogenic microorganisms. *Proc. Natl Acad. Sci. USA* **95**, 3140–3145 (1998).
62. Sanfilippo, C. M., Haas, W., Hesje, C. K. & Morris, T. W. in *Association for Research in Vision and Ophthalmology (ARVO)* (Fort Lauderdale, 2012).
63. Aziz, R. K. *et al.* The RAST Server: rapid annotations using subsystems technology. *BMC Genomics* **9**, 75 (2008).
64. Delcher, A. L., Harmon, D., Kasif, S., White, O. & Salzberg, S. L. Improved microbial gene identification with GLIMMER. *Nucleic Acids Res.* **27**, 4636–4641 (1999).
65. Finn, R. D. *et al.* The Pfam protein families database. *Nucleic Acids Res.* **36**, D281–D288 (2008).
66. Li, L., Stoeckert, Jr. C. J. & Roos, D. S. OrthoMCL: identification of ortholog groups for eukaryotic genomes. *Genome Res.* **13**, 2178–2189 (2003).
67. Guindon, S. *et al.* New algorithms and methods to estimate maximum-likelihood phylogenies: assessing the performance of PhyML 3.0. *Syst. Biol.* **59**, 307–321 (2010).

68. Corander, J., Waldmann, P., Marttinen, P. & Sillanpää, M. J. BAPS 2: enhanced possibilities for the analysis of genetic population structure. *Bioinformatics* **20**, 2363–2369 (2004).
69. Zankari, E. *et al.* Identification of acquired antimicrobial resistance genes. *J. Antimicrob. Chemother.* **67**, 2640–2644 (2012).
70. Keller, L. E. *et al.* Draft genome sequences of five multilocus sequence types of nonencapsulated *Streptococcus pneumoniae*. *Genome Announc* **1**, pii: e00520-13 (2013).

## Acknowledgements

Portions of this project were supported by NIH grants EY024285, Molecular Basis for Ocular Surface Tropism in Conjunctivitis and by the Harvard-wide Program on Antibiotic Resistance, AI083214. HHSN272200900018C supported the involvement of A.M.M. Additional support for this project was obtained from the ALSAC organization of St Jude Children's Research Hospital (J.W.R., C.B., R.A.C. and E.I.T.). In addition, portions of this project were supported by Bausch and Lomb Inc. (C.M.S., W.H., T.W.M. and M.S.G.). M.D.V. was supported in part by NIH fellowship through EY007145. P.J.M.B. was supported by a grant from the Coordenação de Aperfeiçoamento de Pessoal de Nível Superior, Brazil (CAPES #9775-13-7). We gratefully thank Drs F. Lebreton, D. Van Tyne and M. Martin for their helpful comments throughout the course of this work and during manuscript preparation. Funding agencies had no role in study design, data analysis, decision to publish or preparation of the manuscript.

## Author contributions

M.S.G. and M.D.V. conceived and designed the study. M.D.V., A.M.M., P.J.M.B., C.B., C.M.S. and R.A.C. performed the experiments. M.D.V., A.M.M., J.W.R. and M.S.G. contributed to the analysis and interpretation of the results. The manuscript was written by M.D.V. and M.S.G. M.E.Z., B.B., T.W.M. and W.H. provided strains from conjunctivitis. A.M.E. and E.I.T. provided additional guidance during manuscript preparation.

## Additional information

**Accession codes:** Draft genome sequences have been deposited in the DDBJ/EMBL/GenBank databases under BioProject PRJNA229402. See Supplementary Data 2 for individual accession codes for the draft genome sequences.

**Supplementary Information** accompanies this paper at <http://www.nature.com/naturecommunications>

**Competing financial interests:** The authors declare no competing financial interests.

**Reprints and permission** information is available online at <http://npg.nature.com/reprintsandpermissions/>

**How to cite this article:** Valentino, M. D. *et al.* Unencapsulated *Streptococcus pneumoniae* from conjunctivitis encode variant traits and belong to a distinct phylogenetic cluster. *Nat. Commun.* **5**:5411 doi: 10.1038/ncomms6411 (2014).